*Korean J. of Chem. Eng.*, 9(4), 212-217 (1992)

# AXIAL MIXING OF RESIN BEADS IN A GAS-SOLID FLUIDIZED BED

**Yong Chil Seo*, Myung Han Ko and Yong Kang**

*Radwaste Treatment Technology Department, Korea Atomic Energy Research Institute
Department of Chemical Engineering, Chungnam National University
*(Received 15 July 1992 • accepted 17 November 1992)*

**Abstract**—As a first stage of studies on the development of a fluidized bed incinerator for radioactive spent ion-exchange resins, the axial mixing characteristics of anion exchange resin beads and glass beads in a fluidized bed were investigated. The extent of axial solid mixing could be well characterized with a diffusion model and a global mixing index under various experimental conditions such as excess air velocities, size differences of particles and concentrations of resins. It was found that a certain extent of mixing or segregation was reached after 90 s. Axial diffusion coefficients are varing from 1 to 5 $cm^2/s$ in this experimental ranges. The best conditions to incinerate anion resin beads with glass beads as bed materials in the gas-solid fluidized bed system, were 30 wt% of resins in overall composition and excess air velocity over 8 cm/s with glass beads having an averaged diameter of 320 μm.

## INTRODUCTION

Spent ion-exchange resin beads generated from nuclear power plants have higher radioactivity and swelling property as a result of water absorption. Most of radioactive wastes have been processed to form solid cement blocks since cementation technology is well developed and is a cheaper process giving appropriate safety. However, cementation technique could not be utilized for treating spent ion exchange resins, because its swelling property causes to the cement be broken and to result in potential leakage of radioactivity into the environment. Therefore many researchers have expended much effort to develop an alternative means of treating such spent resins, which would provide ample stability in the final product. Incineration, especially fluidized bed incinerators, could be one useful alternative to treat these spent resins since resins are quite easy to feed continuously and have some fluidity with uniform shape and size. Research and development has been performed by several researchers [1, 2] and a commercialized incinerator has been constructed for miscellaneous wastes [3].

KAERI (Korea Atomic Energy Research Institute) has built a bench-scale fluidized bed incinerator. As a related basic experiment, the mixing characteristics of spent resins which are lighter materials (specific gravity: 1.16) than bed materials (sands or glass beads) in a fluidized bed has been studied to find a proper mixing ratio and feed rate of resins. The mixing behavior in a fluidized bed was observed with various excess gas velocities, particle size and density and averaged compositions of mixture. Such experimental results were analyzed by using an axial diffusion model and a mixing index.

*To whom all correspondences should be addressed.

## MIXING MODELS

In this study two mixing models, a mixing index and a diffusion model, were applied to observe mixing extent in the axial direction during fluidization.

### 1. Mixing Index and Global Mixing Index

The overall weight fraction of tracer or combustive materials (resins generally in this study) in total mixture and the local weight fraction at a certain point i, are defined as X and $X_i$, respectively. Then, the mixing index ($IM_i$) is described as follows [4, 5];

$$IM_i = X_i/\overline{X} \tag{1}$$

if $IM_i = 1$, represents perfect mixing, and if $IM_i = 0$ or $1/\overline{X}$, represents perfect segregation. In case the experiment is initiated in a totally segregated condi-

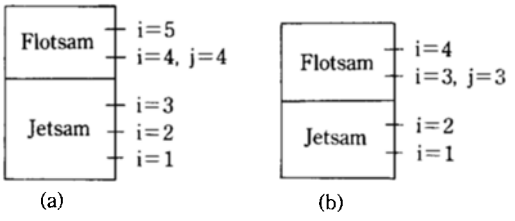


**Fig. 1. Initial particle distributions before fluidization.**

tion, the initial particle distribution is shown in Fig. 1. In the segregation and mixing of fluidizing particles the relatively denser and bigger particles tend to fall down and the lighter and smaller particles move upward in a fluidized bed. The former and later particles used to be called as jetsam and flotsam, respectively. The initial condition as shown in Fig. 1, could be expressed as follows;

for $i \geq j$ (at flotsam layer)

$$IM_i^o = 1/\overline{X} \tag{2}$$

for $i < j$ (at jetsam layer)

$$IM_i^o = 0 \tag{3}$$

where $IM_i^o$ is a local mixing index at initial condition, i is the layer number of the sampling point and j is the layer number of the first sampling point in the flotsam section from the distributor. When the number of layers is N, each layer is assumed to have uniform mixing and the sampling is perfect, the averaged mixing index of flotsam is unity. Then the standard deviations could be described at initial condition and at time t during fluidization as follows;

$$S = \left[\frac{1}{N-1}\sum_{i=1}^{N}(IM_i - 1)^2\right]^{1/2} \tag{4}$$

$$So = \left[\frac{1}{N-1}\sum_{i=1}^{N}(IM_i^o - 1)^2\right]^{1/2} \tag{5}$$

And the global mixing index is, then, defined as a function of above standard deviations [6-9],

$$IMG = 1 - (S/S_o) \tag{6}$$

$$= 1 - \left[\frac{\frac{1}{N-1}\sum_{i=1}^{N}(IM_i - 1)^2}{\frac{1}{N-1}\sum_{i=1}^{N}(IM_i^o - 1)^2}\right]^{1/2} \tag{7}$$

In order to apply such expression to this experimental initial condition, the equation could be described by combining with Eqs. (2) and (3).

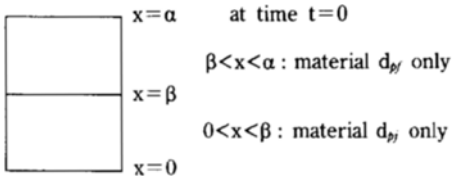


**Fig. 2. Representation of fluidized bed.**

$$IMG = 1 - \left[\frac{\sum_{i=1}^{N}(IM_i - 1)^2}{\left(\frac{1}{\overline{X}} - 1\right)^2 N_j + (N_t - N_j)}\right]^{1/2} \tag{8}$$

where, $N_t$ is the total number of sampling points, $N_j$ is the number of sampling points in flotsam section. The values of global mixing index (IMG) is varying between 0 and 1, which shows perfect segregation and mixing, respectively.

## 2. Axial Diffusion Model

A general unsteady state diffusion model could be applied to understand mixing degree in a fluidized bed. Differences in both sizes and densities could be resin variables to affect to the mixing and segregation in fluidized bed, and some diffusion and mixing index models in the literatures [10-15] were mainly used to observe such influence. Considering one dimensional diffusion in axial direction, the diffusion model is simply expressed as follows;

$$\frac{\partial C}{\partial t} = D\frac{\partial^2 C}{\partial X^2} \tag{9}$$

with initial and boundary conditions as shown in Fig. 2.

$$C = 1 \text{ at } t = 0,\ x > \beta \tag{10a}$$

$$C = 0 \text{ at } t = 0,\ x < \beta \tag{10b}$$

$$C = \overline{C} \text{ at } t = \infty,\ x > 0 \tag{10c}$$

$$\frac{\partial C}{\partial x} = 0 \text{ at } t > 0,\ x = 0 \tag{10d}$$

$$\frac{\partial C}{\partial t} = 0 \text{ at } t > 0,\ x = \alpha \tag{10e}$$

Equation was solved with given initial and boundary conditions and the final solution is,

$$\therefore C - \overline{C} = \frac{-2}{\pi}\left\{\frac{\mathrm{SIN}\left(\frac{\pi}{\alpha}\beta\right)}{1}\exp\left[-\left(\frac{\pi}{\alpha}\right)^2 Dt\right]\left(\mathrm{COS}\frac{\pi}{\alpha}x\right) + \frac{\mathrm{SIN}\left(\frac{2\pi}{\alpha}\beta\right)}{2}\exp\left[-\left(\frac{2\pi}{\alpha}\right)^2 Dt\right]\left(\mathrm{COS}\frac{2\pi}{\alpha}x\right)\right.$$

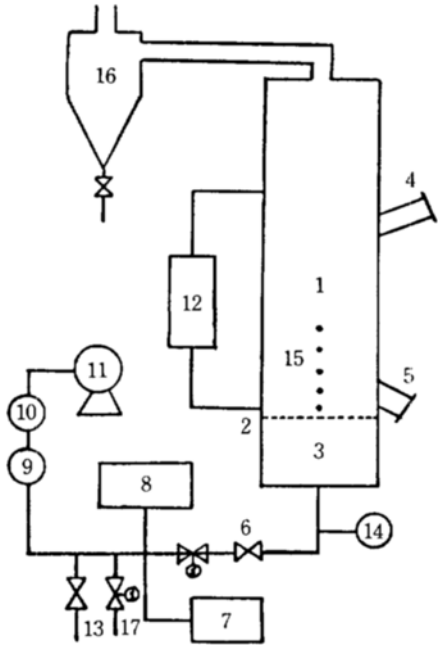


**Fig. 3. Experimental apparatus.**

1. Fluidized bed
2. Distributor
3. Air box
4. Solid loading port
5. Solid discharge
6. Control valve
7. Inclined manometer
8. Anemometer
9. Air filter
10. Air regulator
11. Root blower
12. Differential manometer
13. By-pass line
14. Pressure gauge
15. Sample port
16. Cyclone
17. Solenoid valves

$$+\frac{\mathrm{SIN}\left(\frac{3\pi}{\alpha}\beta\right)}{3}\exp\left[-\left(\frac{3\pi}{\alpha}\right)^2 Dt\right]\left(\mathrm{COS}\frac{3\pi}{\alpha}x\right)+\cdots\cdots\Big\} \quad (11)$$

Using this equation, D could be estimated from the measured values of concentration, C, in different location at a certain time, t.

## EXPERIMENT

A schematic diagram of the experimental apparatus is shown in Fig. 3. The fluidized bed was fabricated with a transparent acryl column (28 cm-ID and 180 cm-high) which simulated the bench-scale fluidized bed incinerator constructed at KAERI. For sampling by using a sample probe at different locations along axial distances (2.8, 6.8, 10.8, 15.8, and 20.8 cm) above the distributor, sampling ports having a size of 0.6 cm were fabricated with attaching adhesive rubber to avoid leakage of bed materials. The air distributor was manufactured using a perforated stainless steel plate (5 mm thick) and the air plenum was 20 cm in height. A cyclone was installed to capture entrained fines. In bed materials glass beads were used for main fluidizing particles as a jetsam in general and anion ion-exchange resin beads for combustive particles as a flotsam. The anion resin beads were dried up to 20-25% of moisture content. The size distributions of particles used in the experiment are listed in Table 1. Each experiment was started from perfect segregation with glass beads as jetsam in the lower section and resin beads as a flotsam in the upper section as an initial condition. Air was injected at a certain flowrate and fluidization mixing was started and stopped by switching on and off both solenoid valves. After defluidization, samples were obtained using a grain sample probe which was a grain sampler type of cylindrical tube (0.6 cm diameter, 35 cm long) to fit into sampling ports. The sampling tube was introduced to the defluidized bed and the mixture of two particles along the radial direction of the bed were sampled. The amount of each sample was about 3-5g and three times of sampling were carried out at one point to abtain enough amount of sample to be representing the averaged mixture along radial distance. The compositions in a sample were analyzed in two means. When the mixture consisted of different particles in size distribution, samples were sieved to find their composi-

**Table 1. Particle size distribution**

| Particle size(μm) | $d_{pi}$ (μm) | Weight fraction($X_i$) | | | | |
|---|---|---|---|---|---|---|
| | | Glass Beads | | | | Anion resins |
| 1000-850 | 925 | 1 | | | | |
| 850-710 | 780 | | 0.0004 | | | |
| 710-600 | 655 | | 0.009 | | | 0.844 |
| 600-500 | 550 | | 0.7594 | 0.0001 | 0.0012 | 0.156 |
| 500-425 | 462.5 | | 0.161 | 0.2606 | 0.0014 | |
| 425-325 | 390 | | 0.0621 | 0.5153 | 0.4568 | |
| 355-300 | 327.5 | | 0.0061 | 0.2101 | 0.3239 | |
| 300-250 | 275 | | 0.002 | 0.0129 | 0.0967 | |
| 250-212 | 231 | | | 0.0008 | 0.0659 | |
| 212-180 | 196 | | | 0.0002 | 0.0213 | |
| 180-150 | 165 | | | | 0.0328 | |
| Harmonic mean diameter(μm) $d_m = 1/\Sigma(x_i/d_i)$ | | 925 | 518.37 | 387.82 | 319.87 | 624.72 |
| Minimum fluidization velocity (cm/sec) | | 28.9 | 14.7 | 10.1 | 7.4 | 8.3 |
| Density(g/cm$^3$) | | | | 2.4671 | | 1.1558 |

**Table 2. Experimental condition**

| | |
|---|---|
| Particle size(μm) | 320-925 |
| Excess air velocity($U-U_{mf}$), cm/sec | 4.16-29.12 |
| Initial weight fraction of the anion resins(%) | 15, 30 |
| Total weight of the fluidized bed(kg) (Glass Beads+Anion Resins) | 15 |

tions. When glass beads and resins were mixed, samples were combusted in oxygen environment using a thermogravimetric analyzer (TGA, LECO MAC-400) because resins were combustible with weight loss in the TGA. The experimental variables and their ranges are shown in Table 2. Size of particles ranged 320-950 μm and the excess air velocity ($U-U_{mf}$) varied as based on jetsam particles with a range of 4-29 cm/s. Fractions of anion resins in total mixture were 15 and 30 wt%. In the different experimental conditions with the above mentioned variables, the compositions along the axial direction of the fluidized bed could be measured and used to estimate local mixing indices, global mixing indices and axial diffusion coefficients to express quantitative mixing extent.

## RESULTS AND DISCUSSION

### 1. Transient Results

Compositions of two particles in a fluidized bed become uniform after reaching a steady state. The main purpose of this study is to observe mixing degree in a steady state, however, the time required to reach a steady state and transient data to prove a diffusion model are important to analyze further information such as mixing degrees and their trends with respect to flowrate, particle characteristics and others. To find out a required time to reach a steady state, which is not changing any more in the averaged composition of the mixture, the sampling and the composition of samples were obtained at 20, 40, 60, 90, 120, 150s after fluidized mixing. Fig. 4 shows the variation of composition with time at different location along the axial distances above the distributor. The mixture in a fluidized bed becomes steady and has uniform compositions at all the locations of the bed after about 60-90s after fluidization. The estimated diffusion coefficient from the experimental results using Eq. (11), that is $D_{ax}=4\ cm^2/s$, could give composition profiles as solid lines in Figs. 4 and 5. It was found that the axial solid mixing rate and degree could be adequately described by diffusion coefficients. Fig. 5 also shows the composition profiles along axial distances at the

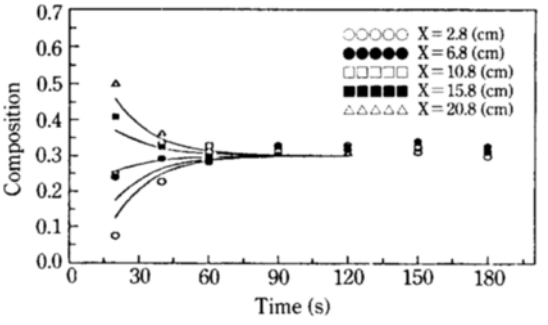


**Fig. 4. Variation of particle composition with time ($D_{ave}=4\ cm^2/s$, $U-U_{mf}=4.16$ cm/s, A30%: G320; resin 30%: Glass bead 320 μm).**

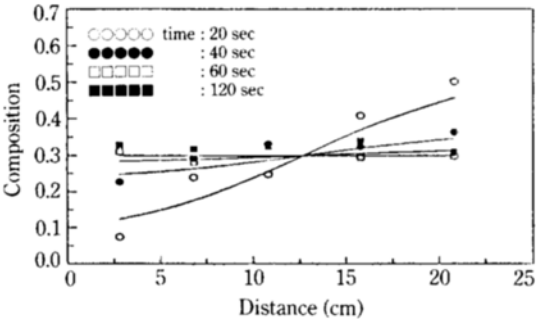


**Fig. 5. Variation of particle composition with axial distance ($D_{ave}=4\ cm^2/s$, $U-U_{mf}=4.16$ cm/s, A30%: G320).**

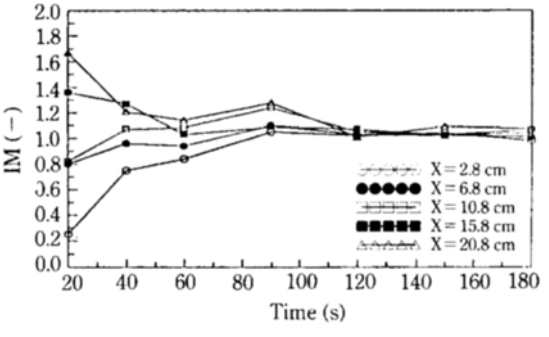


**Fig. 6. Local mixing index with respect to time ($D_{ave}=4\ cm^2/s$, $U-U_{mf}=4.16$ cm/s, A30%: G320).**

same experimental conditions. The local mixing index could also be analyzed by using Eq. (1) and is shown in Fig. 6. In case of this experiment, the mixing index is close to unity and constant with time and shows the a certain extent of mixing or segregation being reached after 90s. Such time is very short and the steady state of the mixing has been reached very fast

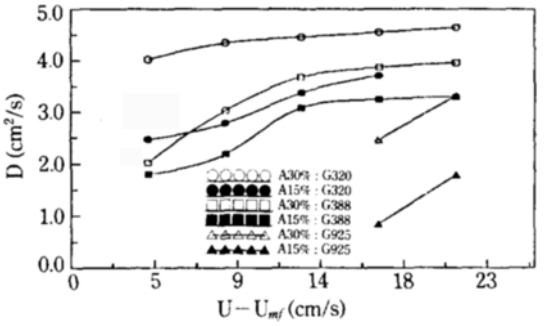


**Fig. 7. Effects of gas velocity on axial diffusion coefficient (A30%: G320, A30%: G388, A30%: G925, A15%: G320, A15%: G388, A15%: G925).**

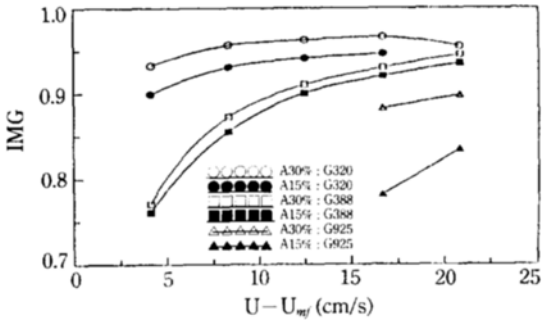


**Fig. 8. Effects of gas velocity on global mixing index (A30%: G320, A30%: G388, A30%: G925, A15%: G320, A15%: G388, A15%: G925).**

in a gas-solid fluidized bed. The results are the same as the analysis made by the axial diffusion in previous model and are similar to other studies [16-18]. The axial diffusion coefficients estimated in the experimental ranges are varying from 1 to 5 $cm^2/s$.

**2. Effect of Overall Composition of Resin Beads**

Nienow et al. [19] has experimented with samll portion of large particles in fluidized bed of smaller ones and Rowe et al. [20], Hemati et al. [8] found that less effects of the concentration of lighter and smaller particles on mixing in a fluidized bed when the gas velocity was twice higher than minimum fluidization velocity. Two different overall compositions, which were 15 wt% and 30 wt% of resin beads, were experimented to observe mixing extent by fluidization. With the same procedures, diffusion coefficients and global mixing indices have been estimated from the obtained experimental results. The estimated values of diffusion coefficients and global mixing indices with excess gas velocities are shown in Figs. 7 and 8.

Diffusion coefficients and mixing indices show higher values at 30 wt% of the overall composition in the mixture than those at 15 wt%. Therefore 30 wt% of the overall composition shows the proper mixing ratio for feeding resin beads into a fluidized bed. From the experience of incinerating resin beads (polymers), the composition of resin beads in waste mixture could not be above 30 wt% due to melting and inadequate combustion such as generating incombustible substance. The 30 wt% of resin beads could be a proper overall composition in mixture and feeding condition for incinerating them.

**3. Effect of Gas Velocity and Particle Size**

It is generally known that the extent of mixing is due to bubble movements [21-24]. The mixing in a fluidized bed is occurred by the movement of bubbles and their wakes. Therefore the increment of bed height is one of the main reasons to form large bubbles and wakes and more vigorous mixing. However, the higher bed height causes to occur slugging. When the ratio of bed diameter to height is around 1, it is found that the enough mixing could be obtain in fluidized beds. Values of solids mixing diffusion coefficients and mixing indices are shown as a function of gas velocity for different bed materials (jetsam) in Figs. 7 and 8. The excess velocity ($U-U_{mf}$) of fluidizing gas ranges up to a velocity of 20 cm/s. Both mixing coefficients and indices increased with excess gas velocities as expected and became constant after a certain gas velocity. The literature [25] showed similar behaviors and the lower values at further higher velocities.

The higher mixing rate was obtained with smaller size jetsam particles. The diffusion coefficient did not become steady when the size of jetsam particles was large (925 μm) even at higher gas velocities. The difference of sizes and densities between two particles caused segregation from each other since the larger and denser particles are falling to the bottom of a fluidized bed. It is generally known that the closer to the unity ratio of two particle sizes is given, the better mixing could be occured with showing higher values of axial mixing diffusion coefficient. Also difference of deneities in two particles is another variable to make more segregation. Therefore, the smaller particle must be denser for better mixing. For combusting ion exchange resin beads at a fluidized bed incinerator, the size of bed materials (sand or glass beads) should be smaller than the size of resin beads. From experimental results, the glass beads having an averaged diameter of 320 μm give the best mixing by such reasons. In these experiments some quantitative mixing could not be described well because two proper-

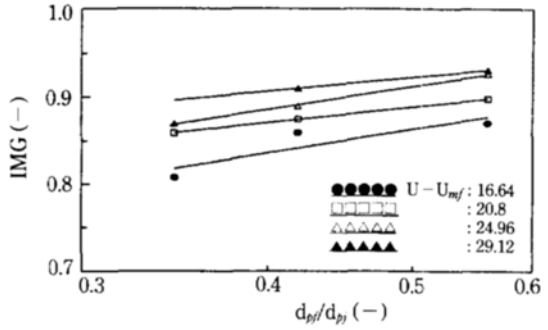


**Fig. 9. Effects of particle size ratio on axial diffusion coefficient (G320: G925, G388: G925, G518: G925).**

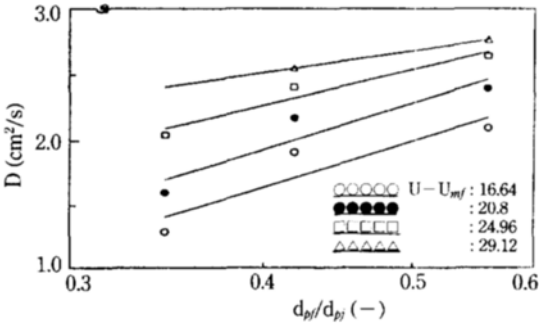


**Fig. 10. Effects of particle size ratio on global mixing index (G320: G925, G388: G925, G518: G925).**

**Table 3. Limited excess air velocity between particle sizes and anion resins**

| Particle size(μm) | Resins(%) | $U-U_{mf}$(cm/s) |
|---|---|---|
| 320 | 30 | ≥8 |
| 388 | 30 | ≥12 |
| 925 | 30 | ≥20 |
| 320 | 15 | ≥8 |
| 388 | 15 | ≥12 |
| 925 | 15 | ≥24 |

ties (size and density) have different and interlocking effects to mixing and segregation of two particles. Further studies will correlate such cross-linked two variables in mixing and segregation at fluidized beds.

Figs. 9 and 10 also show that the diffusion coefficients and mixing indices are a function of the particle size ratio of glass beads. Larger difference of particle sizes makes segregation as shown in the figures.

As a summary of the results in this study, the appropriate conditions for obtaining better mixing extent were listed in Table 3. The overall resin content in a mixture fluidized bed could be 30 wt% rather than 15 wt% in weight. However, excess air velocities must be more than 8, 12 and 20 cm/s for bed materials of glass beads with sizes of 320, 388 and 925 μm, respectively. The best conditions to mix resin beads with glass beads as bed materials in experimented ranges of this gas-solid fluidized bed, were 30 wt% of resins in overall composition and the excess air velocity over 8 cm/s with using glass beads having a diameter of 320 μm.

## CONCLUSIONS

(1) The diffusion model and mixing index model could describe the axial mixing extent in gas-solid fluidized beds. For experimental ranges performed between glass beads and resin beads in this study, the steady state mixing was reached within 90s.

(2) The higher mixing extent was observed with higher overall composition in the mixture. The overall composition in mixture was good enough to combust when the fraction of resin beads was 30 wt% in weight.

(3) Both diffusion coefficients and indices increased with excess gas velocities and became constant after a certain gas velocity. The differences of sizes and densities between two particles caused segregation having lower diffusion coefficients and mixing indices.

## ACKNOWLEDGEMENT

This work was supported by Radioactive Waste Management Fund.

## NOMENCLATURE

D : axial diffusion coefficient of solids [$cm^2$/s]
$\overline{X}$ : mass fraction of flotsam in the bed
IM = $IM_i$ : local mixing index of layer i, demension-less
$X_i$ : mass fraction of flotsam in layer i, [$=m_{fi}/(m_{fi}+m_{ji})$]
$IM_i^o$ : the local mixing index in the i layer before fluidization
S : mixing index based on mass fraction of layers a divided bed, dimensionless
$S_o$ : value of s in the initial situation, i.e. perfect segregation, dimensionless
N : number of layers
$N_t$ : the total number of sampling port
$N_f$ : the number of sampling port in the flotsam layers
C : concentration, fractional weight

$\bar{C}$ : concentration of the flotsam at steady state, fractional weight
t : time [s]
x : axial direction [cm]

**Greek Letters**

α : the total of height of fixed bed [cm]
β : height of jetsam particle [cm]

**Subscripts**

s : solid
g : gas
t : total
f : flotsam
j : jetsam
i : i-th layer

## REFERENCES


1. Valkianien, M.: "Incineration of Ion Exchange Resins in Fluidized Bed", IAEA-R-2358-F (1980).
2. Wirster, W. and Lahner, H. J.: "Test with Ion Exchange Resins in the Incineration Facility of the KFA", Techniche Pruefgesellschaft Lehmann mbh, Berlin (1983).
3. Long, S. W.: "The Incinerator of Lower Level Radioactive Waste", NUREG-1393 (1990).
4. Rowe, P. N., Nienow, A. W. and Agbim, A. J.: *Trans. Inst. Chem. Engr.*, **50**, 324 (1972).
5. Chiba, S., Nienow, A. W., Chiba, T. and Kobayashi, H.: *Powder Technol.*, **26**, 1 (1980).
6. Michaels, A. S. and Puzinauskas, V.: *Chem. Eng. Progr.*, **50**, 604 (1954).
7. Fan, L. T. and Chang, Y.: *Can. J. Chem. Eng.*, **57**, 88 (1979).
8. Hemati, M., Spieker, K., Laguerie, C., Alvarez, R. and Riera, F. A.: *Can. J. Chem. Eng.*, **68**, 768 (1990).
9. Kim, J. R. and Kim, S. D.: Proceedings of the 3rd Asian Conference on Fluidized Bed & Three-Phase Reactors, p. 679, May 1992, Kyungju, Korea (1992).
10. Brodsky, R. B. and Hershey, H. C.: "Transport Phenomena", McGraw, New York (1988).
11. Wwn, C. Y. and Fan, L. T.: "Models for Flow Systems and Chemical Reactors", Marcel Dekker Inc., New York (1975).
12. Mickley, H. S., Sherwood, K. and Reed, C. E.: "Applied Mathematics in Chemical Engineering", 2nd ed., McGraw-Hill, New York (1979).
13. Alkis, C.: "Applied Numerical Methods with Personal Computers", McGraw-Hill, New York (1988).
14. Gibilaro, L. G. and Rowe, P. N.: *Chem. Eng. Sci.*, **29**, 1403 (1974).
15. Bilbao, R., Lezaun, J., Menendez, M. and Izquierdo, M. T.: *Powder Technol.*, **68**, 31 (1991).
16. Shrikhande, K. Y.: *J. Sci. Industr. Res.*, **14b**, 457 (1955).
17. Rowe, P. N. and Nienow, A. W.: *Powder Technol.*, **15**, 14 (1976).
18. Strijbos, S.: *Powder Technol.*, **6**, 337 (1972).
19. Nienow, A. W., Rowe, P. N. and Chiba, T.: *AIChE Symp. Ser.* No. 176, **74**, 45 (1978).
20. Rowe, P. N., Nienow, A. W. and Agbim, A. J.: *Trans. Inst. Chem. Eng.*, **50**, 310 (1972).
21. Kunii, D., Yoshida, K. and Levenspiel, O.: *Ind. Eng. Chem. Fundam.*, **8**, 402 (1969).
22. Kunii, D. and Levenspiel, O.: "Fluidization Engineering", John Wiley, New York (1969).
23. Haines, A. K. and King, R. P.: *AIChE J.*, **18**, 591 (1972).
24. Park, W. H., Kang, W. K., Capes, C. E. and Osberg, G. L.: *Chem. Eng. Sci.*, **24**, 851 (1969).
25. Gabor, J. D.: *Chem. Eng. Prog. Symp. Series* No. 76, **62**, 35 (1966).